Pure & Appl. Chem., Vol.53, pp.1505-1518.
Printed in Great Britain.

0033-4545/81/081505-14$02.00/0
Pergamon Press Ltd.

MODULUS OF THREE AND FOUR FUNCTIONAL POLY(DIMETHYLSILOXANE) NETWORKS

Christopher W. Macosko and Grant S. Benjamin

Department of Chemical Engineering and Materials Science, University of Minnesota, Minneapolis, Minnesota 55455, USA.

Abstract - Networks formed from α, ω divinyl poly(dimethylsiloxane) end-linked with tri- and tetrafunctional hydrosilanes are used to test several theoretical relations for the small strain modulus. The results indicate that topological interactions between chains have a large influence on the modulus, however, the suppression of junction fluctuation by topological interactions seems to be small for PDMS networks. Independent measurement of the topological interactions between chains, the plateau modulus G_N^o on linear PDMS, agrees well with that determined from the networks. The influence of hydrosilane side reactions on determination of network structure parameters was accounted for.

INTRODUCTION

Recently, there has been considerable interest in testing the relation between molecular structure and the theory of rubber elasticity. Of particular concern has been the influence on mechanical properties of topological interactions between network chains. Below we review the various approaches to this problem in terms of the small strain modulus.

If there are no topological interactions, i.e. if the network strands can pass through each other like "phantoms", then the "phantom network" theories of rubber elasticity apply (1-3). For these theories the shear modulus for networks formed and tested in bulk becomes

$$G = (\nu-\mu)RT \tag{1}$$

where ν and μ are the concentrations of elastically active strands and junctions. A junction is elastically active if three or more of its arms are independently attached to the network. A strand is elastically active if it is attached at both ends to an active junction (4). If all strands are attached and there is only one type of junction with functionality f, then $\mu = 2\nu/f$. Thus for a perfect tetrafunctional network Eq. 1 becomes

$$G = 1/2\ \nu RT \tag{2}$$

which is a result that has often been compared to experimental data in the past (5,6). Likewise, for a perfect trifunctional network

$$G = 1/3\ \nu RT \tag{3}$$

In the phantom network, junctions can fluctuate about their mean position due to Brownian motion. This gives rise to the $-\mu$ term in Eq. 1. The higher the junction functionality, f, the less will be the fluctuations. One manifestation of topological interactions may be to suppress the magnitude of these fluctuations (7,8). If all junction fluctuation is suppressed then

$$G = \nu RT \tag{4}$$

which is also the result obtained directly from the assumption of affine deformation. To allow for intermediate behavior Dossin and Graessley have used (9)

$$G = (\nu - h\mu)RT \tag{5}$$

where h is an empirical parameter between 0 and 1.

Another approach is to consider that topological interactions can not only suppress junction fluctuation but also can raise the free energy of deformation further, as if there were additional crosslinks in the network. The idea originates from the observation that linear polymers of high molecular weight behave very much like a crosslinked rubber network over a wide time scale in stress relaxation and other dynamic mechanical tests (10,11). This plateau modulus, G_N^o, appears to be characteristic of the polymer backbone independent of chain length. The plateau modulus is taken to be a measure of topological interactions or entanglements between chains. If the chains are crosslinked, it has been proposed that a

portion of the interactions which contribute to the plateau modulus will not relax out and this will increase the network modulus. Langley (12) and Graessley and coworkers (9, 13) have suggested that these trapped entanglements can be simply added to the small strain modulus from Eq. 5

$$G = (\nu - h\mu)RT + G_N^o T_e \quad (6)$$

where T_e is the proportion of the maximum concentration of topological interactions, G_N^o, which are permanently trapped by the network. Experimentally G_N^o depends on the square of polymer concentration which indicates that it arises from pairwise interactions between chains (10-12). Thus, T_e can be viewed as the probability that a pairwise interaction is made up of elastically active strands.

In order to make a careful test of these various relations between network structure and modulus independent measurements of G and the network parameters ν, μ and T_e as well as the plateau modulus, G_N^o, are required. G can readily be measured by small strain tensile tests on the networks themselves. G_N^o can be determined from dynamic mechanical measurements on high molecular weight linear chains of the same repeat structure as the network strands. Independent determination of the network parameters has been a problem with a number of model network studies. It requires careful characterization of the network precursors, some information on how the network is formed and accurate sol fraction measurements. With these results branching theory can be used to determine ν, μ and T_e (14,15).

In this paper we describe such measurements on poly(dimethylsiloxane) networks formed by end linking α,ω-divinyl PDMS of different molecular weights with three and four functional hydrosilanes. Our results are then used to test the modulus relations given above.

EXPERIMENTAL

Characterization of reactants

We used the platinum catalyzed reaction of multifunctional hydrosilanes to endlink various length α,ω-divinyl PDMS chains (16-20). The reactants are described in Table 1.

TABLE 1. Reactants

Designation	Formula	M_n	Purity	
		formula	(GC)	titration
A_2	$(H\ Si(CH_3)_2O)_2\ Si(Ph)_2$	323	0.95	—
A_3	$(H\ Si(CH_3)_2O)_3\ Si\ Ph$	331	0.986	0.98
A_4	$(H\ Si(CH_3)_2O)_4\ Si$	329	0.954	0.95
B_2	$(Vi\ Si\ Ph\ CH_3)_2O$	324	0.955	—
		titration		M_w/M_n (GPC)
$B_{2,\bar{3}}$	$Vi\ Ph\ CH_3SiO(Si(CH_3)_2O)_n\ SiCH_3\ Ph\ Vi$	3,280		2.1
$B_{2,\bar{4}}$	"	4,190		2.2
$B_{2,\bar{5}}$	"	5,430		2.2
$B_{2,\overline{11}}$(a)	"	11,400		2.3
$B_{2,\overline{22}}$	"	22,400		2.3
$B_{2,\overline{40}}$	"	39,900		2.3
$B_{2,30}$(b)	$Vi(CH_3)_2SiO(Si(CH_3)_2O)_n\ Si(CH_3)_2\ Vi$	30,000(c)		1.1

(a) Starting material for preparation of other $B_{2,\bar{n}}$ samples: Source - Dow Corning Corporation.
(b) Anionically polymerized: Source - K.O. Meyers (22).
(c) M_n = 29,500 by infrared Vi determination, 29,900 by GPC, 33,600 by Vi titration and M_w = 29,700 by light scattering (22,23).

The low molecular weight compounds were either obtained pure from Dow Corning Corporation or vacuum distilled. Purity was measured on a Hewlett-Packard 5730A gas chromatograph. Mercuric acetate titration (21) verified that the impurities were nonreactive.

Several different molecular weight α, ω-divinyl PDMS samples were prepared by reacting one sample of vacuum stripped PDMS M_n = 11,400. Lower M_n was achieved by reequilibration in the presence of the low molecular weight B_2 and a basic catalyst, ammonia (24). The 22,400 and 39,900 samples were prepared by chain extension with A_2 and the platinum catalyst. The 30,000 sample was prepared by anionic polymerization (22). It has a narrow molecular weight distribution and two methyl groups adjacent to each vinyl end group. By contrast the broad distribution samples have a methyl and a phenyl group as indicated in Table 1. The number of end groups was determined by titration (21). The M_n values in Table 1 represent an average of at least 8 determinations. On $B_{2,30}$ these values were in agreement with near infrared vinyl analysis (Cary 14, ref. 22), gel permeation chromatography, GPC (in toluene, Waters Model 200) and low angle laser light scattering (in toluene, Chromatix, KMX-6).

GPC was used to determine the molecular weight distributions. A typical trace for the broad distribution sample is shown in Fig. 1. Note the low molecular weight shoulder. When a network formed from this sample is extracted, a large peak appears in this same position indicating that this material contains no vinyl groups. Meyers (22) has confirmed this by near infrared analysis. From areas under GPC curves and sol fraction measurements, the unreactive material constitutes 2.8 wt% of all the broad B_2 samples. This was confirmed independently on the $B_{2,11}$ samples by Meyers (22). GPC and vapor phase osmometry (in toluene, Wescan Model 232A) on this sample gave lower M_n values than the titration. The difference could be approximately accounted for by 2.8% of a species with M_n = 1200. This weight was too high to be removed by vacuum stripping; however, fractionation should be effective for future work. The narrow distribution sample showed no evidence of unreactable chains. The agreement between endgroup and other M_n determinations indicates that the reactive material was essentially all difunctional.

Hydrosilation chemistry

The catalyst was bis(diethyl)dichloro platinum (II) prepared according to ref. 25. It was dissolved in toluene making a 1 wt% solution and was used at 40 ppm Pt in the reaction mixture to catalyze the hydrosilation.

The main reaction of hydrosilane is

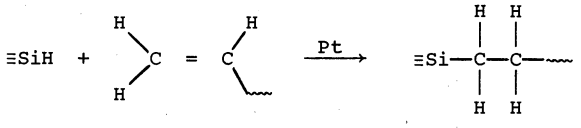

(7)

with model compounds Chalk and Harrod (26) report that this reaction goes to 90% completion. Noll (27) also indicates that platinum can catalyze the reaction of SiH with water

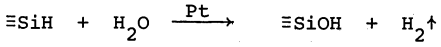

(8)

We have qualitatively confirmed the occurrence of the above reaction by detecting H_2. Hickey has measured quantitatively the rate of disappearance of SiH via infrared (23) with $B_{2,11}$ and platinum, the network formation reaction and at the same initial concentration in pure PDMS. As can be seen from Fig. 2 the rate for side reactions of SiH appears to be much slower than the main reaction. However, at complete conversion of SiH to products, the side reactions consume 5-10% of the SiH (23). This was confirmed by our sol fraction results, discussed below.

We attempted to reduce the side reaction by carrying out the polymerization in an anhydrous N_2-purged glove box. Little difference was observed (23). More exhaustive drying procedures may be required since at the low concentration of SiH used to form our networks 10 ppm of water could be significant. Hickey (23) has shown that other side reactions can occur such as SiH + SiOH and SiOH + SiOH but these appear to be much slower than the water reaction. All the silane should be consumed before SiOH reactions can become important. There is no evidence of any side reactions involving the vinyl group even up to 200°C (22,28).

Network formation and testing

Networks were prepared as follows: 7 grams of the B_2 oligomer was weighed into a clean glass medicine vial, then degassed at 90°C,0.01 atm for 15 min. Though bubbling was observed during this period of degassing, no measurable weight changes occurred. The

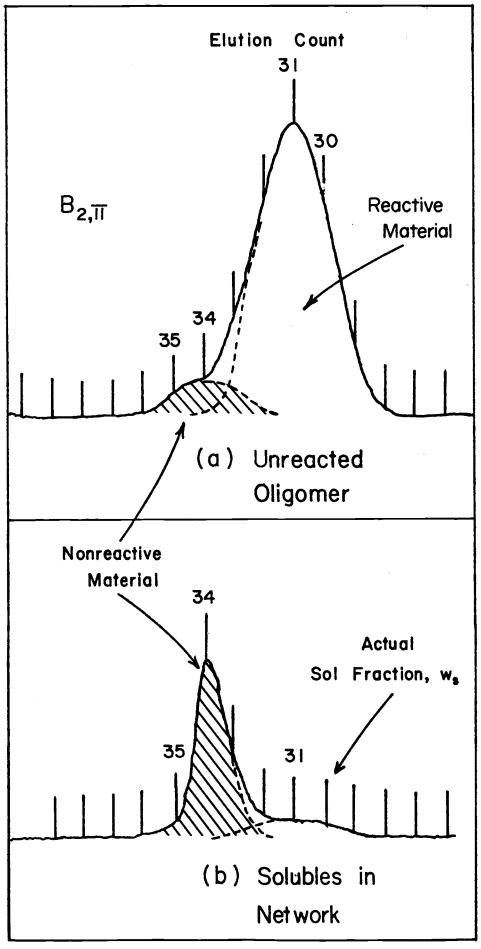

Fig. 1 GPC traces of (a) the unreacted $B_{2,\overline{11}}$ oligomer and (b) the sol fraction from a network formed with this sample; $A_4 + B_{2,\overline{11}}$, r = 1.1. The shoulder at M ≃ 1200 is apparently nonreactive and about 2.8 wt% of the total sample.

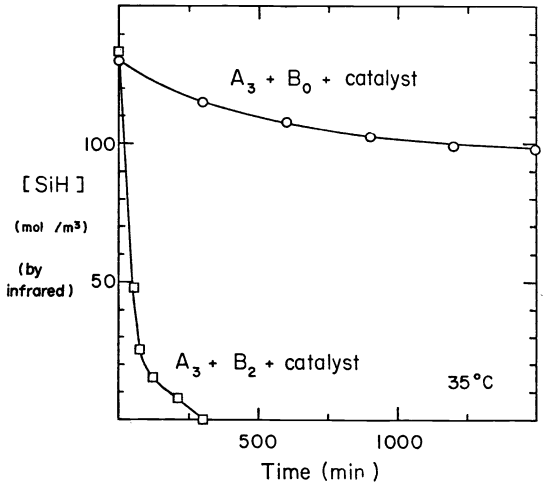

Fig. 2 Rate of disappearance of SiH groups in the presence of pure PDMS and with α, ω divinyl PDMS, 30 ppm of platinum catalyst (23). Meyers reports similar data (22).

degassed B_2 was then reweighed, and crosslinker was added by weight. The crosslinker and oligomer were then stirred mechanically for 5-10 minutes, after which 5 drops of a 1 wt% solution of catalyst was added and mixed for another 5 minutes. The mixture was then poured into a rectangular mold made from Teflon. The mold was then covered and allowed to stand 1 h at room temperature, then for 12 h at 80°C.

The resulting network film, measuring 2×20×140 mm, was used to cut a tensile bar (ASTM D412, type A). Fiducial marks were placed 45 mm apart on the neck of the bar. Thickness was measured using a disk micrometer. The tensile bar was hung vertically, and various weights hung from a clamp on the end. Elongations were measured with a cathetometer 5 minutes after application of the stress. Careful measurements showed that the sample equilibrated in less than 30 seconds after application of the stress, and remain unchanged for 5 days.

Small strain modulus was determined from the slope of a plot of f/A_o vs. $\lambda - 1/\lambda^2$, where f is tensile force, A_o original cross section and λ is extension ratio. Data for λ between 1.0 and 1.1 were used to determine the slope. This was divided by 3 to give the equilibrium shear modulus, G. These results were generally 0-5% higher than the low strain extrapolations from Mooney Rivlin plots of the large strain data. G values also compared well to several disk samples measured in step and dynamic shear using a Rheometrics Mechanical Spectrometer (29,30). We estimate the G values reported below to have a standard deviation of ±3%.

After testing the tensile bars were placed in 250 ml of toluene to obtain sol fraction data. These samples were held in sealed jars at ambient temperature for 6 days. Except for GPC studies of the sol fraction, the toluene was exchanged every 24 hours. No weight change was observed after 4 days. Parallel sol fractions, for examination by GPC, were also taken by extracting 1 g of a thin film in 100 ml of toluene for 7 days. Swollen weight was recorded and then the networks were allowed to evaporate to constant weight. From repeated measurements on pieces of the same film sol fraction measurements should have a standard deviation of less than ±0.0005. For all the w_s data on networks made from the broad distribution oligomers, $B_{2,\bar{n}}$, the fraction of unreactive species 0.028 has been subtracted.

Plateau modulus G_N^o was determined from sinusoidal shear measurements, G' and G", on several high molecular weight linear PDMS samples using a Rheometrics Dynamic Spectrometer. The parallel plate mode with 2-5 mm thick samples and 10% maximum dynamic strain was used. Frequency sweeps were carried out in the automated mode from 0.01 to 500 rad/s from -20°C (near the crystallization temperature of PDMS) to +150°C. Weight average molecular weight was measured by low angle laser light scattering.

TABLE 2. Determination of G_N^o on linear PDMS

Source	M_w Light Scattering $\times 10^6$	G'_{plat} $\times 10^5$ Pa	$G''_{max}/0.207$ $\times 10^5$ Pa	$\frac{2}{\pi}\int_{-\infty}^{\infty} G''d\ell n\omega$ $\times 10^5$ Pa
Bioleau (31)	9.9	2.4	2.32	(2.48)
Weitz (32)	2.1	2.4	2.18	2.23
Meyers (33)	0.95	—	1.79	1.85
Weitz (32)	0.26	—	1.88	(1.80)

RESULTS

Plateau modulus

Four high molecular weight linear PDMS samples were obtained from several sources. Their M_w values are given in Table 2. All the samples were believed to have relatively narrow molecular weight distributions, < 2.0. The 10^7 molecular weight sample has such a long relaxation time that it handled very much like our rubber networks. It appears to have retained its general shape for several years. We cut and sanded it into a disk 3.9×9.5 mm for the dynamic testing and as of this writing, 3 months later, the razor-blade marks are only now beginning to disappear. The only obvious mechanical difference between this high molecular weight linear sample and crosslinked networks is that it is less brittle; it can be extended to very high deformation before rupture. Yet, it totally dissolved in toluene after about 4 weeks. The solution can be passed through a 0.5 μm syringe filter, albeit with

difficulty.

The other samples could be molded to a 25 mm diameter disk under gravity. With the 2.1×10^6 sample it took over a week for the bubbles to rise out. The dynamic mechanical data are given in Fig. 3. There are three methods for obtaining G_N^o from these data (24). The most direct is to measure the plateau in G'. A plateau was measurable for the two highest

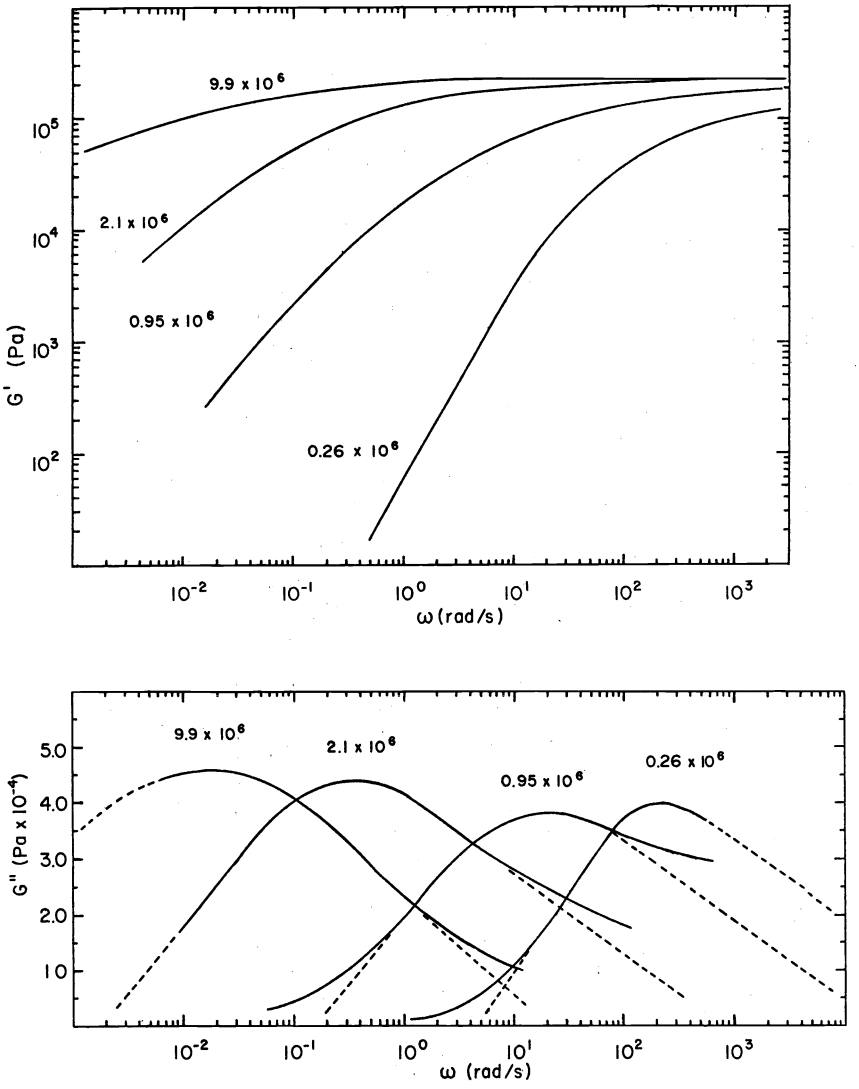

Fig. 3 Dynamic mechanical moduli of four high molecular weight linear PDMS samples. Dotted lines extrapolation for eq. 10 integration.

M_w samples but not accessible for the lowest. For samples where a plateau is not clearly identifiable, Ferry (23, p. 404-407) recommends the correlation with the peak in G"

$$G_N^o = G''_{max}/0.207 \tag{9}$$

or the area under the G" vs. $\ell n\omega$ curve

$$G_N^o = \frac{2}{\pi}\int_{-\infty}^{\infty} G''d\ell n\omega \tag{10}$$

The latter method requires extrapolation of the G" data to zero. From Table 2 we see that all three of these methods are in good agreement for the two highest M_w samples. From these results, G_N^o for PDMS is $2.4 \pm 0.2 \times 10^5$ Pa. This lies between the two literature values 2.0 (34) and 2.9 (35) and we believe it represents the most accurate data available.

Network parameters

To test the influence of network structure on modulus we must have accurate measures of the network parameters: ν, the concentration of elastically active strands, μ, the concentration of active junctions and T_e, the probability that both chains involved in a topological interaction are active strands. If the endlinking reaction is perfect, then ν can be calculated from the average length of the starting chains

$$\nu = \frac{\rho RT}{M_n} \tag{11}$$

and as indicated in the Introduction μ depends on ν and the junction functionality

$$\mu = 2\nu/f \tag{12}$$

Since ideally all strands will be active parts of the network, then $T_e = 1$.

A number of previous studies have assumed perfect endlinking and used the relations above. This can be dangerous because ν and T_e are particularly sensitive to slight incompleteness in the endlinking. For the hydrosilation reaction used here, clearly the side reaction will cause incomplete network formation. However, ν, μ and T_e can still be calculated using branching theory. The key experimental quantity required is the conversion of SiH and vinyl groups to links, p_{SiH} and p_{Vi}. Ideally, we would like to measure SiH, Vi and their product $SiCH_2CH_2$ or Et directly such as spectroscopically. Although SiH is readily measured with infrared, its concentration will always be nearly zero due to the side reaction. As for the Vi and Et groups, we have not yet found a method to accurately measure their concentration in formed networks.

Another approach to measuring the number of links formed is to use sol fraction data. If both ends of a B_2 oligomer are not reacted into the network, then it can be removed by swelling. Miller and Macosko (14) have derived relations between sol fraction w_s and the conversion of endgroups. For networks formed from $A_3 + B_2$

$$w_s = w_{A_3}\left(\frac{1 - rp^2}{rp^2}\right)^3 + w_{B_2}\left(\frac{rp^3 + 2rp^2 - 1}{rp^3}\right)^2 \tag{13}$$

and

$$r = [A]_o/[B]_o = [SiH]_o/[Vi]_o \tag{14}$$

where $p = p_{SiH}$ the extent of reaction of SiH groups with Vi and $rp = p_{Vi}$ extent of the Vi groups. Since r is known from the initial concentrations of reactants, then from sol fraction measurements we can use eq. 13 to determine p_{SiH} and p_{Vi}. This is shown graphically in Fig. 4. For example, for about 0.2% sol and $r = 1.1$, the relative conversion of SiH groups is 0.90 and Vi is 0.98. These results can then be used in relations for ν, μ and T_e. For example, for $A_3 + B_2$ networks

$$\nu = \frac{3}{2}[A_3]_o\left(\frac{2p_{SiH}\,p_{Vi} - 1}{p_{SiH}\,p_{Vi}}\right)^3 \tag{15}$$

Thus, for a network with 0.2% sol and $r = 1.0$ ν will be reduced to about 88% of its value at complete endlinking, $\nu = [A_3]_o$. For μ we use 2/3 ν on trifunctional networks and

$$T_e = \left(\frac{2p_{SiH}\,p_{Vi} - 1}{p_{SiH}^2\,p_{Vi}}\right)^4 \tag{16}$$

The same approach can be used on the four functional networks. Figure 5 gives the relation between w_s and r and p_{Vi} and p_{SiH} for $A_4 + B_2$ systems. Here about 0.05% sol and $r = 1.1$ indicates that $p_{SiH} = 0.90$ and $p_{Vi} = 0.98$. All equations for tetrafunctional network parameters are given in ref. 14 and 18.

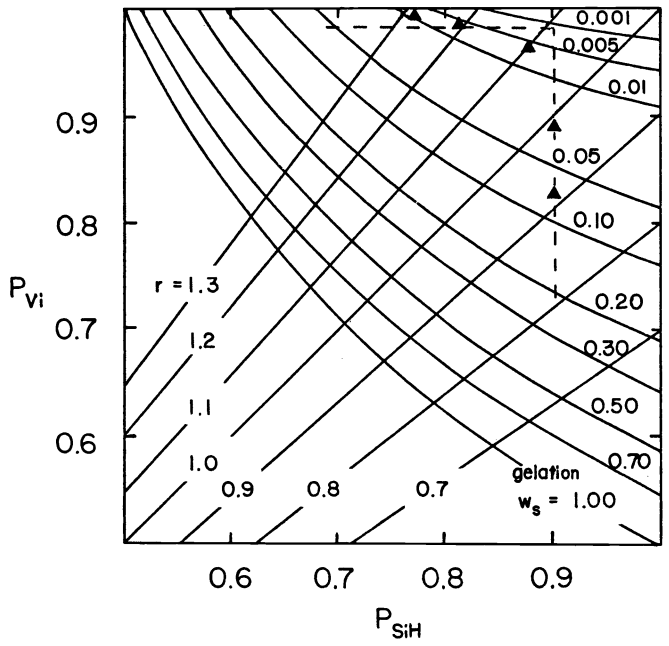

Fig. 4 Sol fraction map for $A_3 + B_2$ endlinked networks. If $w_s = 0.002$ and the stoichiometric ratio r is 1.1, then the fraction conversion of SiH to network links is 0.90 and of Vi is 0.98. Triangles indicate experimental points from Table 3 also plotted in Fig. 6.

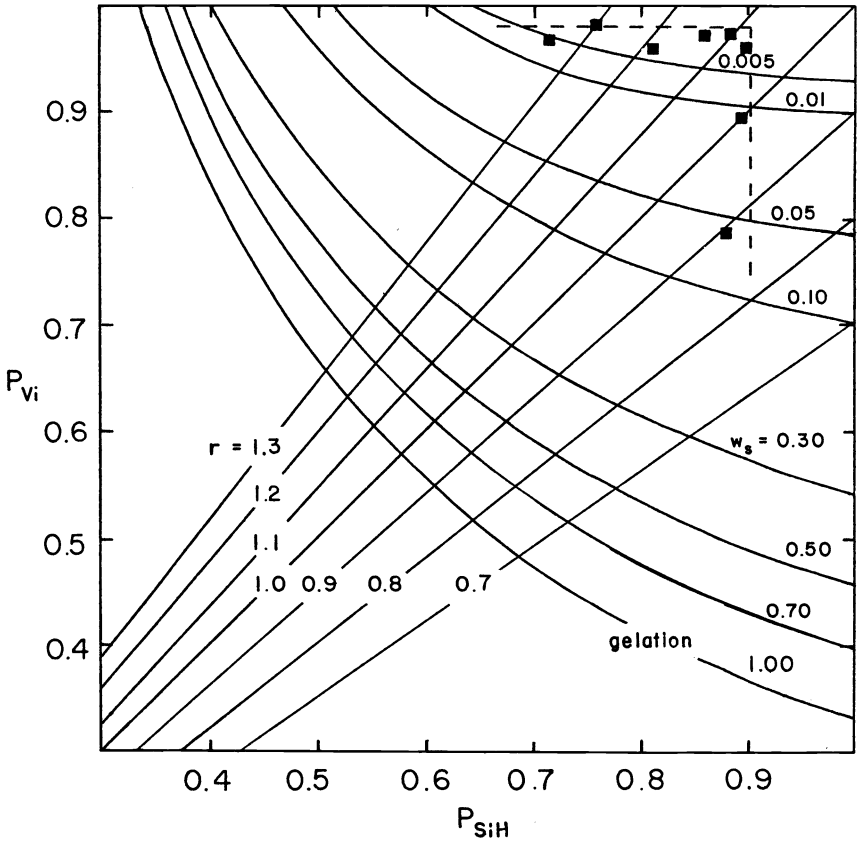

Fig. 5 Sol fraction map for $A_4 + B_2$ endlinked networks. Squares are experimental points from Table 4 also plotted in Fig. 7.

All our sol fraction data is given in Tables 3 and 4 along with the calculated network parameters and the small strain modulus data. We have indicated the w_s points for the $B_{2,11}$ system on Figs. 4 and 5. Although there is some scatter for $r \lesssim 1.1$, it appears that the conversion of SiH to network linkages, Eq. 7, is limited to 0.90 for both tri- and tetrafunctional crosslinker. This limit appears to be due to the side reaction, Eq. 8. The experimental scatter may be due to variation in water contamination between runs. At high r the reaction becomes limited by vinyl conversion which appears not able to exceed 0.98. This may be due to steric problems.

TABLE 3. Trifunctional endlinked PDMS networks

$\overline{M}_n$	r	w_{sol}	G ($\times 10^5$ Pa)	T (K)	p_{SiH}	νRT ($\times 10^{-5}$ Pa)	T_e	$\frac{G}{T_e}$	$\frac{\nu RT}{T_e}$
39,900	0.99	0.102	0.448	299.0	0.841	0.111	0.214	2.09	0.52
		0.103	0.527	297.0	0.841	0.111	0.214	2.46	0.518
30,000	1.09	0.0325	1.12	302	0.835	0.281	0.451	2.48	0.624
	1.21	0.0358	0.975		0.777	0.245	0.435	2.24	0.563
	1.29	0.0367	1.02		0.745	0.228	0.430	2.37	0.530
22,400	0.998	0.076	0.608	298	0.851	0.249	0.275	2.21	0.903
		0.073	0.622	285.5	0.853	0.246	0.284	2.19	0.864
11,400	0.913	0.079	0.65	298.5	0.899	0.508	0.265	2.45	1.92
	0.998	0.0314	1.24		0.889	0.812	0.460	2.69	1.77
	1.11	0.0073	1.93		0.861	1.11	0.690	2.80	1.61
	1.21	0.0060	1.92		0.814	1.07	0.731	2.63	1.46
	1.31	0.0040	2.21		0.775	1.05	0.783	2.82	1.34
	0.988	0.0381	0.979	293.5	0.887	0.732	0.419	2.34	1.75
		0.0369	0.961	298	0.888	0.752	0.430	2.27	1.78
	1.11	0.0106	1.26	295.5	0.855	1.03	0.650	1.94	1.60
	1.34	0.0055	1.82		0.759	0.956	0.743	2.45	1.29
5,430	0.986	0.119	0.62	297.5	0.835	0.680	0.182	3.39	3.74
4,190	0.987	0.0497	1.47	297.5	0.876	1.69	0.362	4.06	4.66
	1.15	0.0255	1.69	290.5	0.813	1.95	0.502	3.37	3.87
	1.25	0.0418	1.25	291.5	0.757	1.45	0.405	3.08	3.58
3,280	1.01	0.0456	1.77	295	0.866	2.16	0.380	4.66	5.68
	1.10	0.0091	2.96		0.864	3.56	0.672	4.41	5.30
	1.20	0.0113	2.57		0.808	3.05	0.643	4.00	4.75
	1.30	0.0252	1.78		0.751	2.23	0.515	3.46	4.34

We illustrate these same $B_{2,11}$ data in Figs. 6 and 7 as w_s vs. r. The solid lines are from the theory assuming $p_{SiH} = 0.90$ up to the p_{Vi} limit of 0.98.

Modulus results

In Figs. 6 and 7 we have also plotted the modulus values. Note that they go through a maximum over the same range that w_s is a minimum. This is to be expected; here will be the highest degree of endlinking, the highest concentration of network strands. If we take these maximum modulus values for networks made from each of the different molecular weight B_2 oligomers and plot them vs. $\rho RT/M_n$, we obtain the results shown in Fig. 8. This would be a correct test of the theoretical relations if we could assume the networks were completely endlinked and is the method used frequently in previous studies. Although we know that ν should actually be somewhat lower for these data, we can see immediately from Fig. 8 that of the theoretical models only Eq. 6 can qualitatively represent the data. As ν goes to zero, G has a finite value indicating interchain topological interactions and the slopes differ between the tri- and tetrafunctional network samples indicating that junction fluctuation is not completely suppressed.

TABLE 4. Tetrafunctional endlinked PDMS networks

M_n	r	w_{sol}	G ($\times 10^5$ Pa)	T (K)	p_{SiH}	νRT ($\times 10^{-5}$ Pa)	T_e	$\frac{G}{T_e}$	$\frac{\nu RT}{T_e}$
30,000	1.11	0.0441	1.31	302	0.760	0.349	0.389	3.37	0.90
	1.20	0.0242	1.46		0.742	0.416	0.507	2.88	0.819
	1.32	0.0213	1.44		0.694	0.403	0.533	2.70	0.756
22,400	1.03	0.0401	1.14	304	0.811	0.519	0.407	2.80	1.27
	1.11	0.0161	1.76		0.807	0.670	0.580	3.03	1.16
	1.21	0.0173	1.60		0.750	0.618	0.571	2.80	1.08
	1.30	0.0162	1.51		0.710	0.590	0.578	2.61	1.02
11,400	1.00	0.0157	2.05	299.5	0.884	1.40	0.582	3.52	2.41
	1.10	0.0025	2.91		0.868	1.74	0.813	3.58	2.14
	1.19	0.0070	2.21		0.787	1.45	0.705	3.14	2.06
	1.33	0.0078	2.28		0.716	1.31	0.694	3.29	1.88
	1.06	0.0034	2.50	298.5	0.892	1.73	0.786	3.18	2.20
	1.13	0.0032	2.62		0.842	1.66	0.791	3.31	2.10
	1.18	0.0014	3.03		0.823	1.73	0.858	3.53	2.01
	1.30	0.0016	2.76		0.755	1.60	0.854	3.23	1.87
	1.13	0.0860	0.93	302	0.712	0.601	0.247	3.77	2.43
	1.17	0.0040	2.95		0.817	1.65	0.796	3.71	2.07
	1.20	0.0029	2.68		0.800	1.63	0.802	3.34	2.03
4,190	1.00	0.0083	3.43	297	0.912	4.20	0.678	5.10	6.20
	1.10	0.0052	3.60		0.851	4.22	0.739	4.87	5.70
	1.20	0.0041	4.61		0.793	4.06	0.765	6.03	5.30
	1.31	0.0037	4.26		0.739	3.86	0.783	5.44	4.92

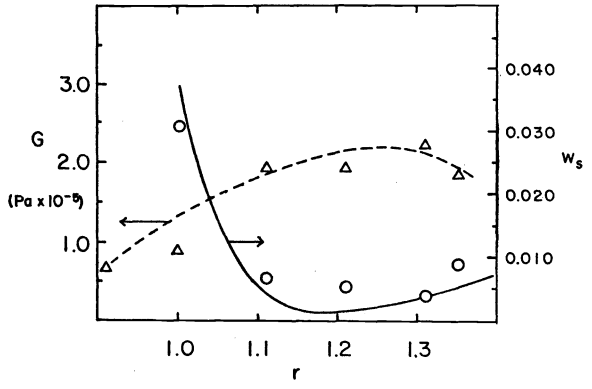

Fig. 6 Sol fraction and modulus for $A_3 + B_{2,11}$ networks formed at various stoichiometric ratios. The solid line is theory (Eq. 13 and Fig. 4) assuming $p_{SiH} = 0.90$ up to the point that $p_{Vi} = 0.98$.

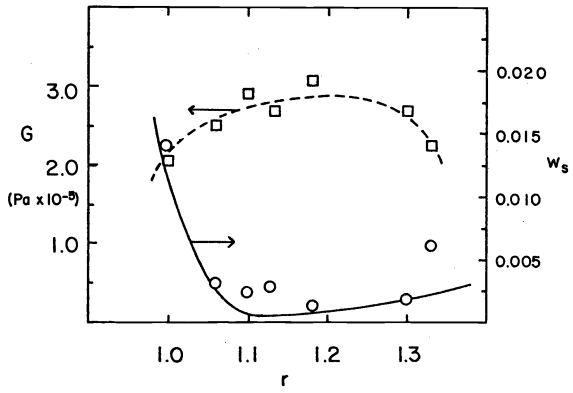

Fig. 7 Sol fraction and modulus for $A_4 + B_{2,\overline{11}}$ networks formed at various stoichiometric ratios. Solid line from Fig. 5 with $p_{SiH} = 0.90$ up to $p_{Vi} = 0.98$.

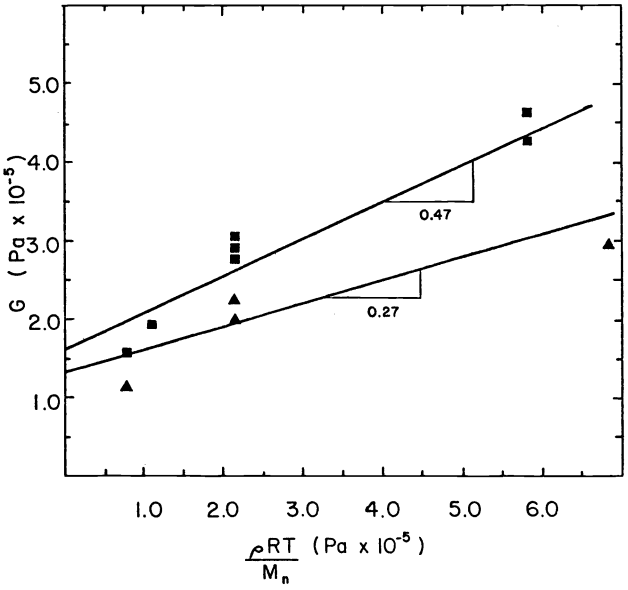

Fig. 8 Small strain modulus vs. reciprocal of oligomer chain length for trifunctional, ▲, and tetrafunctional, ■, samples with lowest sol fraction, $w_s < 0.01$, and thus most complete reaction.

In Figs. 9 and 10 we plot all the tri- and tetrafunctional samples now taking into account incomplete endlinking, the last two columns of Tables 3 and 4. Despite the range of stoichiometric ratio, sol fraction and molecular weight of the B_2 materials, the results are surprisingly consistent. As expected, accounting for the reduction in ν and T_e due to incomplete reaction increases the intercepts and slopes from Fig. 8. For the trifunctional networks, the intercept is $2.01 \pm 0.07 \times 10^5$ Pa, slightly less than G_N^o. The slope is 0.37 ± 0.04; 0.33 would be expected for no suppression of junction fluctuations, h=1. For the tetrafunctional junctions the agreement with eq. 6 is quantitative. The intercept

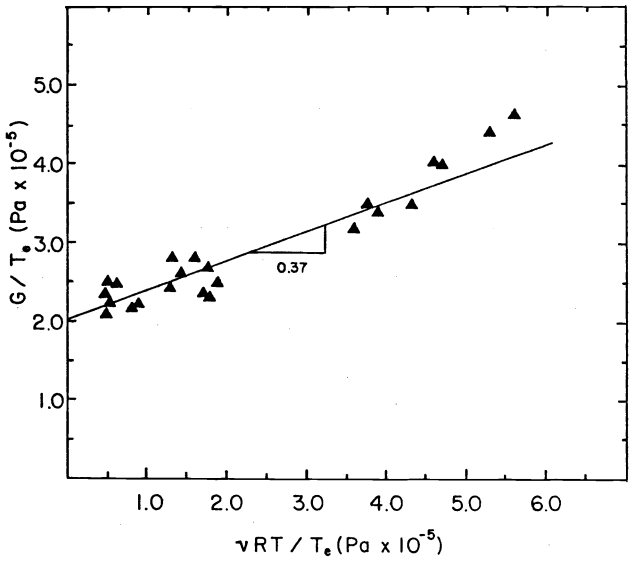

Fig. 9 Small strain modulus vs. concentration of elastically active strands reduced by the factor T_e for all trifunctional samples. In calculating ν and T_e, incompleteness of endlinking has been accounted for.

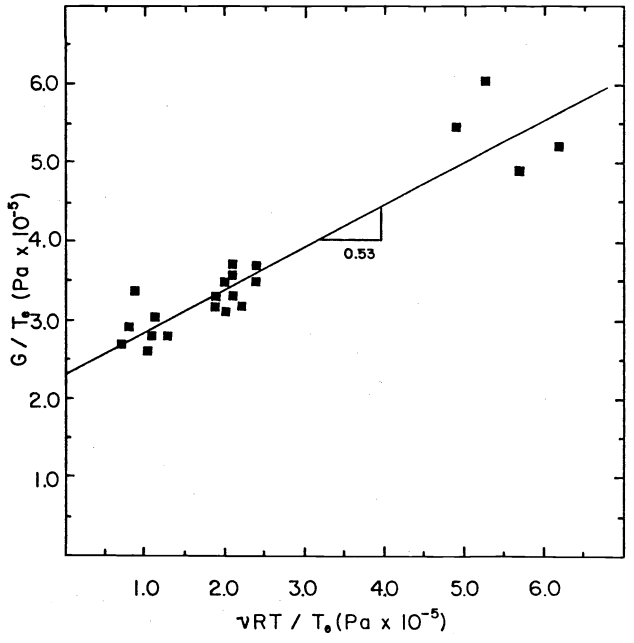

Fig. 10 Same as Fig. 9 for all tetrafunctional samples.

$2.34 \pm 0.05 \times 10^5$ Pa is within the uncertainty on G_N^o. The slope 0.53 ± 0.1 again indicates little suppression of junction fluctuations. However, for incomplete endlinking with a tetrafunctional crosslinker, some of the junctions will be three functional. This could mask a small influence of topological interactions on junction fluctuation.

CONCLUSIONS

In this study we have summarized the presently available models relating the small strain modulus of rubber to its network structure. To test these models we have attempted to measure independently the modulus, network structure parameters and a chain interaction parameter on endlinked poly(dimethylsiloxane) networks. We found that there is a small but significant side reaction of the SiH functional crosslinks used for the endlinking. The effect of this side reaction and a small incompleteness in vinyl conversion can be properly accounted for by making sol fraction measurements. Studies on the nature of these hydrosilation reaction are continuing in our laboratory.

Our results can be best explained by a network model which includes the effect of topological interactions between chains. The magnitude of this effect is equal to that measured for linear PDMS, the plateau modulus. There does not appear to be much suppression of junction fluctuations by the topological interactions. As recently reviewed by Gottlieb et al. (36) these results are in agreement with essentially all other small strain modulus data on model silicone networks when incomplete linking is properly accounted.

Small strain modulus is an important part of the total stress strain response of rubber. Our work continues into large strain of these model networks.

Acknowledgement - This research was supported by a grant from the Army Research Office. We are pleased to acknowledge N. R. Langley and T. Maxson of Dow Corning Corporation and E. W. Merrill and K. O. Meyers of Massachusetts Institute of Technology for providing materials. We are also indebted to them and M. Gottlieb for helpful discussions during the course of the work.

REFERENCES

1. W. W. Graessley, Macromolecules 8, 186 (1975).
2. K. J. Smith, Jr. and R. J. Gaylord, J. Polym. Sci., Phys. Ed. 13, 2069 (1975).
3. P. J. Flory, Proc. Roy. Soc. London Ser. A351, 351 (1976).
4. J. Scanlan, J. Polym. Sci. 45, 397 (1960).
5. P. J. Flory, Principles of Polymer Chemistry, Cornell University Press, New York (1953).
6. L. R. G. Treloar, The Physics of Rubber Elasticity, 3rd ed., Clarendon Press, Oxford (1975).
7. G. Ronca and G. Allegra, J. Chem. Phys. 63, 4990 (1975).
8. P. J. Flory, J. Chem. Phys. 66, 5720 (1977).
9. L. M. Dossin and W. W. Graessley, Macromolecules 12, 123 (1979).
10. J. D. Ferry, Viscoelastic Properties of Polymers, 2nd ed., Wiley, New York (1970).
11. W. W. Graessley, Ad. Polym. Sci. 16, 1 (1974).
12. N. R. Langley, Macromolecules 1, 348 (1968).
13. D. S. Pearson and W. W. Graessley, Macromolecules 13, 000 (1980).
14. D. R. Miller and C. W. Macosko, Macromolecules 9, 206 (1976).
15. D. S. Pearson and W. W. Graessley, Macromolecules 11, 528 (1978).
16. E. M. Valles and C. W. Macosko, Rubber Chem. Technol. 49, 132 (1976); A.C.S. Div. Org. Cont. and Plastics Preprints 35(2), 44 (1975); in Networks: Structure and Properties, S. S. Labana, Ed., Academic Press, p. 401 (1977).
17. E. M. Valles and C. W. Macosko, Macromolecules 12, 521 (1979).
18. E. M. Valles and C. W. Macosko, Macromolecules 12, 673 (1979).
19. M. A. Llorente and J. E. Mark, J. Chem. Phys. 71, 682 (1979).
20. M. A. Llorente and J. E. Mark, Macromolecules 13, 681 (1980).
21. A. L. Smith, Analysis of Silicones, Wiley Interscience, New York (1974).
22. K. O. Meyers, Ph.D. Thesis, Department of Chemical Engineering, Massachusetts Institute of Technology, Cambridge, Massachusetts, April 1980.
23. W. J. Hickey, M.S. Thesis, University of Minnesota, Department of Chemical Engineering and Materials Science, Minneapolis, Minnesota, 1980.
24. A. J. Barry and H. N. Beck, in Inorganic Polymers, F. Stone and W. Graham, Eds., Academic Press (1962).
25. C. B. Kaufmann and D. O. Cowan, Inorganic Synthesis, Vol. 6, McGraw-Hill, New York (1969).
26. A. J. Chalk and J. F. Harrod, J. Am. Chem. Soc. 87, 16 (1965).
27. W. Noll, Chemistry and Technology of Silicones, p. 87, Academic Press, New York (1968).
28. T. Maxson, Dow Corning Corporation, personal communication.
29. M. Gottlieb, C. W. Macosko and T. Lepsch, to be submitted.
30. S. Granick, S. Pederson and J. D. Ferry, University of Wisconsin, private communication.
31. S. Boileau, Coll. de France, Paris; sample supplied by E.W. Merrill of Massachusetts Institute of Technology.

32. A. Weitz, Dow Corning Corporation.
33. K. O. Meyers, Massachusetts Institute of Technology, Cambridge, Massachusetts. For synthesis see ref. 22.
34. D. J. Plazek, W. Dannhuser and J. D. Ferry, J. Colloid Sci. 16, 101 (1961).
35. N. R. Langley and J. D. Ferry, Macromolecules 1, 353 (1968).
36. M. Gottlieb, C. W. Macosko, G. S. Benjamin, K. O. Meyers and E. W. Merrill, Macromolecules, submitted.